CSMA 2017
13ème Colloque National en Calcul des Structures
15-19 Mai 2017, Presqu'île de Giens (Var)

A strong fluid/structure coupling scheme for thin incompressible flow in the contact interface at the roughness scale

A. G. Shvarts[1], V. A. Yastrebov[1], G. Cailletaud[1]

[1] *MINES ParisTech, PSL Research University, Centre des Matériaux, CNRS UMR 7633, BP 87, 91003 Évry, France*
{andrei.shvarts, vladislav.yastrebov, georges.cailletaud}@mines-paristech.fr

Résumé — We develop a strong coupling scheme for the mechanical contact and the interfacial thin fluid flow problems. The scheme is applied for simulations on the microscopic level by taking into account roughness of the surfaces with the objective to obtain relevant macroscopic constitutive equation for transmissivity in sealing applications. The problem of trapped fluid is studied in detail : the monolithic coupling scheme is developed for mechanical contact affected by the pressurized fluid trapped in the wavy interface. Results on the evolution of the real contact area, maximal frictional force and global coefficient of friction are presented.
Mots clés — mechanical contact, fluid/structure coupling, surface roughness, trapped lubricant

1 Introduction

Natural and industrial surfaces always have roughness under certain magnification, and the contact in most applications occurs on separate patches corresponding to asperities of the surfaces [1, 2]. The evolution of the real contact area under increasing external load determines essential contact properties, such as friction, wear, adhesion, but also it strongly affects heat and mass transport in and through contact interfaces.

We consider here the problem of coupling the mechanical contact with the thin fluid flow in the interface between the contacting surfaces. On the one hand, the boundary value problems for fluid transport depends on the solution of the mechanical contact problem. On the other hand, the solution of the latter in turn is influenced by the hydrostatic and hydrodynamic pressures of the fluid, which results in the strong coupling between these two problems.

We use the multiscale approach : by performing simulations with the roughness of the contacting surfaces taken into account at microscale, we are able to refine the existing models of the considered phenomenas at the macroscopic scale, which are relevant for such industrial applications, as problems of contact seals and mixed lubrication. The former one is essential for aeronautic, automotive and nuclear industries, and these applications demand generalization of the solution of the coupled problem at the microscopic scale for the macroscopic scale using the roughness-dependent leakage laws. The mixed lubrication is crucial for systems in which either relative sliding velocity between the components can be rather low (starting of rotation in gear boxes, bearings, turbines, etc.) or can reverse (e.g. in pistons), or the external pressure is sufficiently high (metal forming). Again, simulations on the microscopic roughness level enable us to refine the existing macroscopic lubrication models.

In recent years, the problem of fluid transport along the contact interface between two solid bodies with representative rough surfaces has received much attention [3, 4]. Preliminary results for simulation of the contact of an elastic 3D body with a rigid plane and incompressible thin fluid flow in the interface are shown in Fig. 1. An example of the morphology of the contact patches is presented in Fig. 1a, and the simulation of the fluid flow through the resulting channels in the contact interface in Fig. 1b. Note that out-of-contact regions completely surrounded by a contact area are easily distinguishable, i.e. some of the contact patches are *non-simply connected*, see Fig. 1c. Therefore, under the increasing external load, applied to the solid body, the fluid may become trapped in these regions, which would inevitably add additional pressure on the contact interfaces and may affect the geometry of the surfaces.

This paper is organized as follows. The 2nd section is devoted to the trapped fluid problem : the framework is developed for monolithic coupling of the mechanical contact problem with pressurized

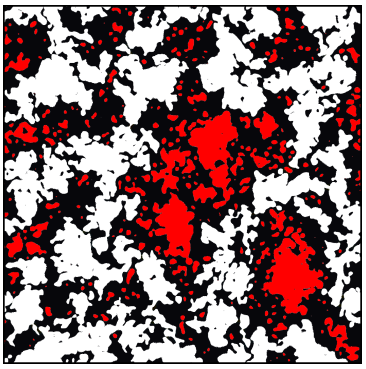

(a)

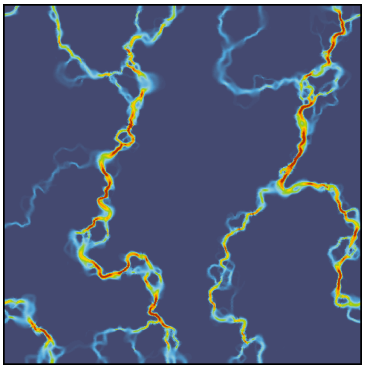

(b)

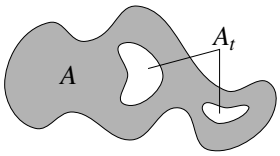

(c)

FIGURE 1 – (a) Morphology of contact patches for the contact of a 3D body with a rigid plane : black is the contact area, white is out of contact and red is "trapped". (b) Incompressible fluid flow through the same contact interface (color represents the flow intensity). (c) An example of non-simply connected contact patch : A is the contact area, A_t is out-of-contact (trapped) area.

fluid trapped in the wavy contact interface, and the real contact area, maximal frictional force and global coefficient of friction evolution under increasing external loading are studied. In the 3rd section different numerical approaches for the fluid/structure interaction are discussed and the problem statement for thin fluid flow through the wavy contact interface is presented. The 4th section summarizes the obtained results.

2 Trapped fluid problem

2.1 Background of the problem

Lubrication is an efficient mechanism of minimizing the direct contact of solids bodies, which consequently reduces friction and wear. However, if the applied external loads, pushing the contacting bodies together, are high enough or if the sliding velocities are small, the asperities of both surfaces can get in contact despite the presence of the lubricant, thus inevitably increasing friction. However, at the same time the lubricating fluid may be trapped in the valleys (pools) between contact patches, which would have a strong effect on the contact properties, especially if the fluid is highly incompressible. First, the trapped fluid resists to compression and thus opposes to the growth of the real contact area. Second, the external load is shared between the contacting asperities of the bodies and the pressurized fluid. Therefore, the integral value of the normal pressure in the contact area is reduced, and, since the maximal tangential frictional stress (in Couloumb's friction law) is proportional to the normal pressure, macroscopic friction coefficient between the two solid bodies is decreasing.

The effect of lubricant trapping on reduction of friction has been first understood in applications for cold metal forming processes [5, 6]. In [7] the regimes of lubrication corresponding to different levels of external pressure are studied, in particular, the escape of the trapped fluid from the pools into the contact area is predicted at sufficiently high loads, a regime when both real contact area and coefficient of friction decrease with increasing load. In [8] experimental results and FEM simulations on the entrapment and escape of the fluid in the contact interface during upsetting of a cylinder are presented.

Kuznetsov [9] proposed an analytical solution for the 2D plane strain problem of contact between an elastic body with a wavy surface and a rigid half-space, taking into account compressible fluid trapped in the valleys between contacting peaks of the wavy profile. Kuznetsov used Westergaard's solution [10, 11] for the contact pressure distribution without influence of the fluid, which is based on the assumption of the small slope of the wavy profile. Kuznetsov's solution describes the reduction of the contact reaction force, compared to Westergaard's solution, and therefore can predict the decrease of the global coefficient of friction. However, due to the assumption of the small slope, it cannot describe the escape of the lubricant and depletion of the real contact area.

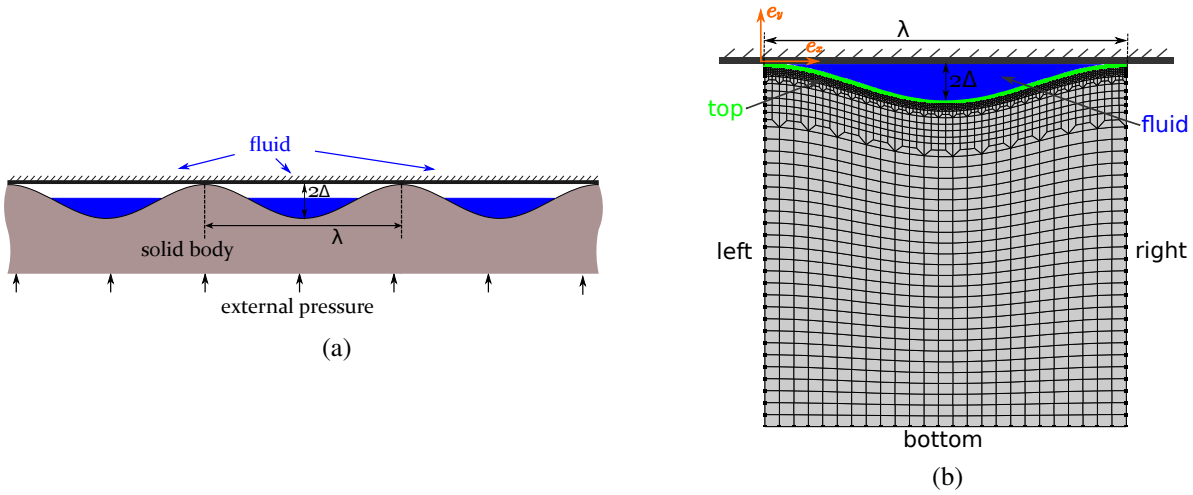

FIGURE 2 – (a) Problem statement. (b) Geometry of the model and example of FE mesh.

2.2 Problem statement

We consider here the mechanical contact problem between a periodic elastic wavy surface and a flat rigid plane (the case which was historically the starting point in the study of contact of rough surfaces [10, 11, 9]) and take into account the influence of compressible or incompressible fluid trapped in the free volume between the two bodies, see Fig. 2a. The geometry of the problem and an example of the structural mesh are presented in Fig 2b, simulations were performed on a FE mesh with 1024 elements on the top surface of the solid body (19364 nodes in total). We assumed the plane strain state and the linear elastic isotropic constitutive law for the solid.

The initial gap between the surface of the body and the rigid plane, as well as the volume of this gap are given by :

$$g(x) = \Delta\left(1 - \cos\frac{2\pi x}{\lambda}\right), \quad V_g = \int_0^{\lambda} \Delta\left(1 - \cos\frac{2\pi x}{\lambda}\right) dx = \lambda\Delta, \tag{1}$$

where Δ and λ are the amplitude and wavelength of the wavy surface profile, respectively.

We apply the symmetry boundary conditions on the vertical walls of the considered solid body and a far-field external pressure p_{ext} or a vertical displacement on the bottom surface.

2.3 Numerical simulation of the coupled mechanical contact/trapped fluid problem using the monolithic approach

2.3.1 Contact constraints

In case of unilateral contact between an elastic deformable body and a fixed rigid plane, the motion of the body is restricted by the plane. This geometrical constraint is formalized upon introduction of the normal gap function g_n - a signed distance from the points on the surface of the deformable body to the rigid plane :

- $g_n > 0$ when the point is separated from the plane (inactive contact state),
- $g_n < 0$ when the point penetrates the plane (which is forbidden),
- $g_n = 0$ when the point is on the plane (active contact state).

We will denote by Γ_c the active contact zone, where the contact pressure σ_n is non-zero. The constraints governing the unilateral frictionless contact problem are known as the Hertz-Signorini-Moreau conditions [12] :

$$g_n \geq 0,\ \sigma_n \leq 0,\ \sigma_n g_n = 0 \quad \text{at} \quad \Leftrightarrow \quad \begin{cases} g_n = 0, & \sigma_n < 0, \quad \text{at}\,\Gamma_c \\ g_n > 0, & \sigma_n = 0, \quad \text{at}\,\Gamma \setminus \Gamma_c. \end{cases} \tag{2}$$

The constrained minimization problem for the energy of the mechanical system $\Pi(\mathbf{u})$, where $\mathbf{u}$ is the displacement field, can be solved using the Lagrange multipliers method [12, 13]. The Lagrangian

function is defined as :

$$\mathcal{L}(\mathbf{u},\lambda^c) = \Pi(\mathbf{u}) + \int_{\Gamma_c} \lambda^c \, g_n(\mathbf{u}) \, d\Gamma_c, \tag{3}$$

where $\lambda^c \leq 0$ is the Lagrange multiplier function, the values of which are equal to the contact pressure.

2.3.2 Geometrical constraint for incompressible fluid

Let us denote by Γ_f the part of the surface of solid body, which interacts with the pressurized fluid. The volume of the gap V_g in the presence of trapped incompressible fluid must satisfy the following geometrical constraint :

$$V_g \geq V_f = \text{const}, \quad V_g(\mathbf{u}) = \int_{\widetilde{\Gamma}_f} g_n(\mathbf{u}) \, d\widetilde{\Gamma}_f, \tag{4}$$

where V_f is the constant volume of the fluid inside the closed trap and $\widetilde{\Gamma}_f$ is the projection of Γ_f on the rigid plane. The trapped fluid may fill completely or partially the gap between the contacting surfaces, therefore it can be present in two different states : "inactive", when $V_f < V_g$ and the fluid if not pressurized, and "active", when $V_f = V_g$, and the fluid is under pressure p_f, see Fig. 3a, 3b. We may formulate this two states in a way similar to Hertz-Signorini-Moreau conditions :

$$V_g \geq V_f, \quad p_f \geq 0, \quad p_f\,(V_g - V_f) = 0 \Leftrightarrow \begin{cases} V_g = V_f, & p_f > 0, \quad \text{(active state)} \\ V_g > V_f, & p_f = 0, \quad \text{(inactive state).} \end{cases} \tag{5}$$

2.3.3 Solution of the coupled problem with the Lagrange multipliers method

In the case of the inactive state of the trapped fluid, we have only the mechanical contact problem between the elastic body and the rigid plane, while if the fluid is in the active state, we must consider additionally the gap volume constraint (4). The Lagrange multiplier method may be used again in order to fulfill this constraint, which defines the combined functional for the coupled problem :

$$\mathcal{L}(\mathbf{u},\lambda^c,\lambda^f) = \Pi(\mathbf{u}) + \int_{\Gamma_c} \lambda^c \, g(\mathbf{u}) \, d\Gamma_c - \lambda^f (V_g(\mathbf{u}) - V_f), \tag{6}$$

where $\lambda^f \geq 0$ is the Lagrange multiplier for the trapped fluid problem, which is equal to the fluid pressure. The solution of the coupled problem is a stationary point of the Lagrangian (6), which requires the calculation of the variation :

$$\delta\mathcal{L}(\mathbf{u},\lambda^c,\lambda^f) = \delta\Pi(\mathbf{u}) + \int_{\Gamma_c} \left[\delta\lambda^c \, g_n(\mathbf{u}) + \lambda^c \, \delta g_n(\mathbf{u})\right] d\Gamma_c - \delta\lambda^f \, (V_g(\mathbf{u}) - V_f) - \lambda^f \, \delta V_g(\mathbf{u}) = 0. \tag{7}$$

To solve this problem, we implemented in FEM framework a monolithic coupling scheme in the framework of the *Z-set* software [14].

2.3.4 Simulation of the compressible fluid using the penalty method

The solution of the discussed problem can also be obtained with the penalty method. At the same time, the formulation under the penalty method is equivalent to considering compressible fluid. In accordance with the linear penalty method, instead of the $\lambda^f (V_g(\mathbf{u}) - V_f)$, the following term should be added

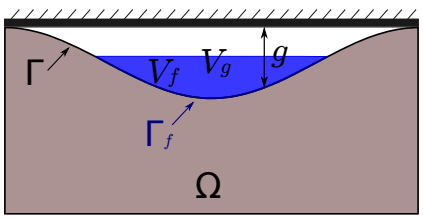

(a) Trapped fluid is in the "inactive" state. g is the normal gap between the contacting surfaces, V_g - volume of this gap, V_f - volume of the fluid.

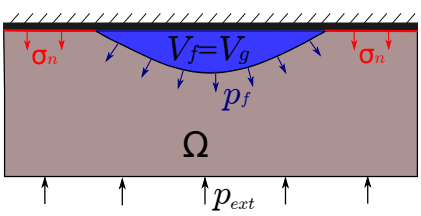

(b) Trapped fluid is in the "active" state, the fluid fills the whole gap volume, p_{ext} is the external pressure, p_f is the fluid pressure, σ_n is the contact normal pressure.

in (6) to take into account the trapped fluid constraint :

$$W_f(\mathbf{u}) = \frac{\varepsilon}{2} \langle V_f - V_g(\mathbf{u}) \rangle^2, \quad \langle x \rangle = \begin{cases} x, & \text{if } x > 0, \\ 0, & \text{if } x \leq 0, \end{cases} \tag{8}$$

where ε is the penalty parameter and $\langle \cdot \rangle$ is the Macauley bracket operator. Let us assume that the fluid is in active state. Calculating the variation of (8), we obtain the contribution of the trapped fluid to the balance of the virtual work :

$$\delta W_f(\mathbf{u}) = \varepsilon \left(V_f - V_g(\mathbf{u}) \right) \delta V_g(\mathbf{u}) = \varepsilon \left(V_f - V_g(\mathbf{u}) \right) \frac{\partial V_g(\mathbf{u})}{\partial \mathbf{u}} \delta \mathbf{u}, \tag{9}$$

where the term $\varepsilon \left(V_f - V_g(\mathbf{u}) \right)$ represents the fluid pressure p_f.

Note that under the penalty formulation, the current volume of the active fluid $V_g(\mathbf{u})$ is always smaller, than the initial fluid volume V_f, which means that the fluid can no longer be considered as incompressible. For the linear penalty method the parameter ε corresponds to the modulus of compressibility K of the fluid – coefficient of proportionality between the change of volume of fluid and the hydrostatic fluid pressure, see [9] : $p = p_0 + K \left(V_0 - V \right) / V_0$, where p_0 is the pressure in fluid, when it has volume V_0, and pressure p corresponds to a smaller volume V. If we assume that initially, when the volume was V_0, the fluid was not pressurized, then the connection between penalty parameter ε and modulus of compressibility of fluid K becomes transparent : $\varepsilon = K / V_f$.

2.4 The influence of the incompressible trapped fluid on the contact problem

Results of our simulations of the coupled contact/trapped fluid problem show, that once the fluid becomes active, the real contact area reaches its maximum value and during the consequent loading is only monotonically decreasing, reaching zero value, i.e. opening the trap, at a certain step of the external loading. In Fig. 4a the evolution of the real contact area is presented for different ratios of the amplitude to the wavelength of the profile (Δ / λ) and different ratios of the initial volume of the fluid to initial gap volume V_f / V_0. It is important to note, that for the case when the fluid fills completely the initial gap volume, the real contact area equals zero during the whole process of loading.

The computational results allow us to estimate the evolution of the value of the global coefficient of friction between an elastic body and a rigid plane under increasing external load affected by the presence of trapped fluid in the interface. We distinguish between global and local coefficients of friction by observing the problem from macroscopic (calculating the reaction forces on the solid body) and microscopic (studying the stress vector components on the rough contact surface) levels respectively. Due to the presence of the pressurized fluid, the macroscopic normal reaction force is the sum of integrals of the normal stress component over the contact and the fluid areas of the interface, while for calculation of the macroscopic tangential reaction force shear forces in the fluid are neglected, since the static friction is considered :

$$|F_n| = \int_{\Gamma_c} |\sigma_n| \, d\Gamma_c + \int_{\Gamma_f} |p_f| \, d\Gamma_f, \quad |F_t| = \left| \int_{\Gamma_c} \sigma_t \, d\Gamma_c \right|. \tag{10}$$

In the above formulas σ_n and σ_t are the normal and tangential components of the stress vector, respectively, and p_f is the fluid pressure. *The global coefficient of friction* is introduced as the coefficient of proportionality between the maximal macroscopic tangential and normal reaction forces : $|F_t^{max}| = \mu_{glob} |F_n|$.

Now let us observe the problem on the microscopic level. We introduce *the local coefficient of friction* by the Coulomb's law : $|\sigma_t| \leq \mu_{loc} |\sigma_n|$. The maximal tangential reaction can be expressed as :

$$|F_t^{max}| = \mu_{loc} \int_{\Gamma_c} |\sigma_n| \, d\Gamma_c. \tag{11}$$

The evolution of the maximal reaction force is presented in Fig. 4b. Finally, we obtain the estimative value of the ratio between global and local coefficients of friction :

$$\frac{\mu_{glob}}{\mu_{loc}} = \frac{\int_{\Gamma_c} |\sigma_n| \, d\Gamma_c}{\int_{\Gamma_c} |\sigma_n| \, d\Gamma_c + \int_{\Gamma_f} |p_f| \, d\Gamma_f}. \tag{12}$$

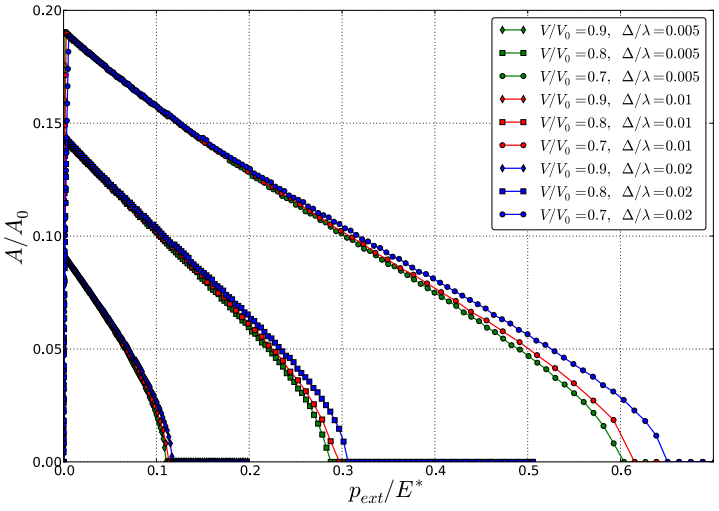

(a)

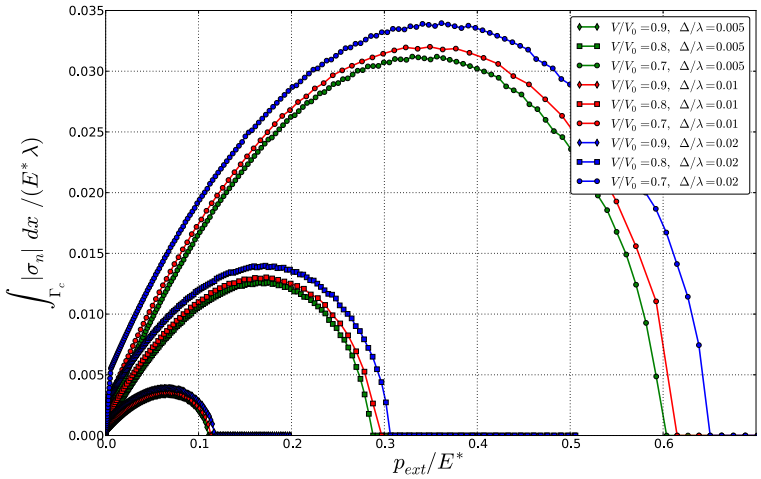

(b)

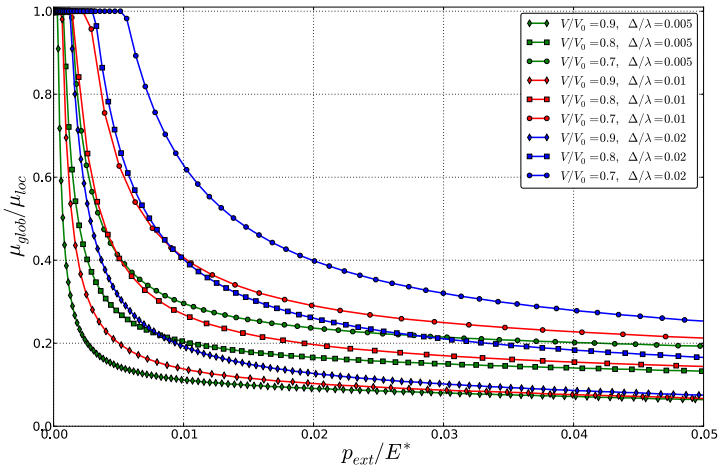

(c)

FIGURE 4 – Evolution of the real contact area (a), the normalized contact normal reaction (b) and the global coefficient of friction (c) with respect to normalized external pressure for different ratios of the amplitude to the wavelength of the profile and different ratios of the initial volume of the fluid to initial gap volume. E^* is the effective elastic modulus of the solid body [11].

From the above formulas it follows that global coefficient of friction is smaller or equal, than the local one : $0 \leq \mu_{glob} \leq \mu_{loc}$. The results on the estimation of the ratio between global and local coefficients of friction are presented in Fig. 4c.

3 Coupling contact problem with thin fluid flow in the interface

3.1 Numerical approaches

Two different approaches of numerical solution of the fluid-structure interaction problem exist :

Partitioned approach : Numerical solvers for the mechanical contact and fluid transport are separated and work sequentially, so that the data exchange between them must be established. Different resolution schemes under this approach exist, in the order of increasing accuracy :

- Unilateral coupling : both problems are solved only once each at every load step, and the mechanical solver provides the fluid solver the geometry of the contact interface, while the influence of the fluid on the mechanical problem is neglected.

- Weak coupling : at every load step the mechanical problem is solved and data is sent to the fluid transport solver, which in its turn solves the problem on updated geometry. At the next load step the mechanical problem is solved with additional pressure coming from the previous load step of the transport solver, however, the convergence of this coupled problem is not ensured.

- Strong coupling : the fluid transport problem is solved on the updated geometry after each iteration of the mechanical problem (the numerical simulation of contact is nonlinear and requires iterative resolution, e.g. Newton-Raphson method), which takes into account the updated value of the fluid pressure, and a convergence criterion is introduced and verified at the end of each load step.

Monolithic approach : The fluid pressure values are added as degrees of freedom (DOFs) to the nodes of the structural mesh, and the surface elements for solving the fluid problem are appended to this mesh. Therefore, the equations governing fluid flow are rendered into the global system of equations, which is solved at each iteration. When a convergence criteria is fulfilled, the solution is obtained for both displacement and fluid pressure fields.

3.2 Problem statement for incompressible flow in the contact interface

The problem of the fluid/structure interaction for the case of the thin fluid flow in the wavy contact interface between a 3D elastic body and a rigid plane (see Fig. 5) can be formulated as the following system of equations and constraints :

$$\begin{cases} \nabla \cdot \underline{\underline{\sigma}} = 0 & \text{in } \Omega \quad (13a) \\ g_n \geq 0,\ p \geq p_f,\ (p - p_f)\, g_n = 0 & \text{on } \Gamma \quad (13b) \\ \nabla \cdot \left[g_n(\underline{\mathbf{u}})^3 \nabla p_f \right] = 0 & \text{in } \Gamma_f \quad (13c) \\ p_f|_{\text{inlet}} = p_i, \quad p_f|_{\text{outlet}} = p_o & \quad (13d) \end{cases}$$

for the unknown displacement field $\underline{\mathbf{u}}$ and a scalar value of fluid pressure p_f. Here $\underline{\underline{\sigma}}$ is the mechanical stress tensor, defined in the solid body Ω, p is the pressure on the wavy surface Γ, g_n is the gap between this surface and the rigid flat, (13a) is the balance of the momentum equation and (13b) are the Hertz-Signorini-Moreau conditions, modified to take into account the external fluid pressure p_f, (13c) is the Reynolds equation for thin isoviscous incompressible flow, and $\Gamma_f \subset \Gamma$ is the part of the surface, which is out of contact. We apply periodic boundary conditions and the external pressure on the rigid flat, and p_i and p_o are the fluid pressure at the inlet and outlet, respectively.

4 Conclusions

We develop in the FEM framework a monolithic resolution scheme for coupling mechanical contact with the thin fluid flow in the interface. This complex problem is split into two sub-problems : the study of the trapped fluid in the contact interface and of the fluid flow through a wavy channel. For both problems strong monolithic coupling schemes are elaborated and implemented in the FEM software Z-set.

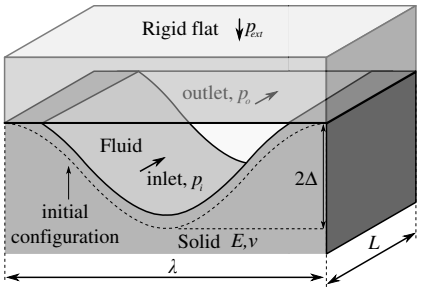

FIGURE 5 – Fluid flow through a periodic wavy contact interface.

We demonstrated that the trapped fluid influence on the solution is more complicated, than it can be predicted analytically under the assumption of infinitively small slope of the roughness profile :

- If the compressibility modulus of the fluid is higher then the one of the solid (e.g. if the fluid is considered incompressible), then once the fluid becomes pressurized, the contact area is monotonically decreasing under increasing external load.

- If the incompressible fluid fills completely the gap between the surfaces, it cannot be trapped.

- If the fluid fills the initial gap partially, the static friction force becomes a non-monotonic function of the applied external pressure, does have a maximum value and decreases to zero value under consequent load.

For the problem of the fluid flow through a wavy contact interface we implement both partitioned and monolithic coupling approaches, compare their performance and verify the results using an approximate analytical solution, which was also derived.

5 Acknowledgments

The authors acknowledge the financial support from MINES ParisTech (Thèse-Open) and Safran Tech. Enriching discussions and help of Julien Vignollet are greatly appreciated.

Références

[1] V. A. Yastrebov, G. Anciaux, and J.-F. Molinari. Contact between representative rough surfaces. *Phys. Rev. E*, 86(3), 2012.

[2] V. A. Yastrebov, G. Anciaux, and J.-F. Molinari. From infinitesimal to full contact between rough surfaces : Evolution of the contact area. *Int. J. Sol. Struct.*, 52 :83–102, 2015.

[3] B.N.J. Persson and C. Yang. Theory of the leak-rate of seals. *J. Phys. : Cond. Matt.*, 20(31) :315011, 2008.

[4] W. B. Dapp, A. Lücke, B. N. J. Persson, and M. H. Müser. Self-affine elastic contacts : percolation and leakage. *Phys. Rev. Lett.*, 108(24) :244301, 2012.

[5] H. Kudo. A note on the role of microscopically trapped lubricant at the tool-work interface. *Int. J. Mech. Sc.*, 7(5) :383–388, 1965.

[6] T. Nellemann, N. Bay, and T. Wanheim. Real area of contact and friction stress — The role of trapped lubricant. *Wear*, 43(1) :45–53, 1977.

[7] A. Azushima and H. Kudo. Direct Observation of Contact Behaviour to Interpret the Pressure Dependence of the Coefficient of Friction in Sheet Metal Forming. *CIRP Annals - Manuf. Tech.*, 44(1) :209–212, 1995.

[8] A. Azushima, A. Yanagida, and S. Tani. Permeation of Lubricant Trapped Within Pocket Into Real Contact Area on the End Surface of Cylinder. *J. Tribol.*, 133(1) :011501, 2011.

[9] Ye.A. Kuznetsov. Effect of fluid lubricant on the contact characteristics of rough elastic bodies in compression. *Wear*, 102(3) :177–194, 1985.

[10] H. Westergaard. Bearing Pressures and Cracks. *J. App. Mech.*, 18, 1939.

[11] K.L. Johnson, J.A. Greenwood, and J.G. Higginson. The contact of elastic regular wavy surfaces. *Int. J. Mech. Sc.*, 27(6) :383–396, 1985.

[12] V. A. Yastrebov. *Numerical methods in contact mechanics*. John Wiley & Sons, 2013.

[13] P. Wriggers. *Computational Contact Mechanics*. Springer Nature, 2006.

[14] `http://www.zset-software.com`, 2016.